Experimental Observation of High-Order Quantum Accelerator Modes

S. Schlunk,[1] M. B. d'Arcy,[1] S. A. Gardiner,[1] and G. S. Summy[1,2]

[1]*Clarendon Laboratory, Department of Physics, University of Oxford, Parks Road, Oxford OX1 3PU, United Kingdom*

[2]*Department of Physics, Oklahoma State University, Stillwater, Oklahoma 74078-3072*

(Received 2 December 2002; published 27 March 2003)

Using a freely falling cloud of cold cesium atoms periodically kicked by pulses from a vertical standing wave of laser light, we present the first experimental observation of high-order quantum accelerator modes. This confirms the recent prediction by Fishman, Guarneri, and Rebuzzini [Phys. Rev. Lett. **89**, 084101 (2002)]. We also show how these accelerator modes can be identified with the stable regions of phase space in a classical-like chaotic system, despite their intrinsically quantum origin.

DOI: 10.1103/PhysRevLett.90.124102 PACS numbers: 05.45.Mt, 03.65.Sq, 32.80.Lg, 42.50.Vk

The search for signatures of chaos and stability in quantum systems whose classical analogs exhibit chaotic dynamics is an area of intense current theoretical and experimental interest [1]. The motivation is twofold. First, the study of how complex classical behavior originates in the quantum regime helps in understanding the operation of the quantum-classical correspondence principle and thus the physical processes that are crucial in determining observed macroscopic behavior, particularly when this behavior is chaotic. Second, the quantum dynamics of such systems are of considerable interest in their own right, especially when the systems behave in a peculiarly nonclassical manner.

Approaches to the classification of (chaotic) quantum behavior have ranged from the highly mathematical (e.g., trace formulas [2]) through the statistical (energy spectra [3]) to the more phenomenological (energy and momentum transfer to ensembles of particles [4]). It is the last approach which is most appealing as a philosophy to guide experiment and underpins the work presented here. Resonant, stable behavior in quantum systems often depends on precise fulfillment of matching conditions between, e.g., periodic forcing of a system and its own natural frequency, in contrast to the looser matching generally required in the corresponding classically chaotic system [5]. The quantum resonances [6] observed in the δ-kicked rotor [7,8] represent an excellent example of this quantum-classical dichotomy. These resonances are characterized by the steady transfer of momentum to the system, which in the atom-optical case [9,10] manifests itself as a symmetric broadening of the atomic momentum distribution for special values of the driving frequency of the potential. Addition of a static linear potential, e.g., due to gravity, realizes the δ-kicked accelerator. The classical dynamics of this system are qualitatively similar to those of the δ-kicked rotor, but the quantum dynamics are quite distinct. This is exemplified by very different quantum resonant behavior, producing quantum accelerator modes (QAM), at values of the driving frequency close to (but not at) those for which quantum resonances occur in the δ-kicked rotor. QAM are characterized by the asymmetric transfer of a fixed momentum impulse per kick to $\sim$20% of the initial ensemble of laser-cooled atoms [11–14]. This resonant behavior was analyzed theoretically by Fishman, Guarneri, and Rebuzzini (FGR) [5], which led to the prediction of the existence of whole families of higher-order QAM.

In this Letter, we report the first experimental observation of these high-order QAM, finding excellent quantitative agreement with the analysis of Ref. [5]. This is achieved using an atom-optical realization [8–10,15] of the quantum δ-kicked accelerator [11–14]. Pulses from a vertical standing wave of laser light are applied to freely falling laser-cooled atoms. The Hamiltonian is

$$\hat{H} = \frac{\hat{p}^2}{2m} + mg\hat{z} - \hbar\phi_d[1 + \cos(G\hat{z})]\sum_n \delta(t - nT). \quad (1)$$

Here $\hat{z}$ is the position, $\hat{p}$ is the momentum, m is the particle mass, g is the gravitational acceleration, t is the time, T is the pulse period, $G = 2\pi/\lambda_{\text{spat}}$, where λ_{spat} is the spatial period of the potential applied to the atoms, and $\hbar\phi_d$ quantifies the depth of this potential. The kicking potential acts on the atoms as a phase grating that induces a phase modulation of amplitude ϕ_d to their de Broglie waves. Hence, the effect of a pulse on a plane wave is to cause diffraction into a series of momentum states separated by the grating recoil $\hbar G$. Between consecutive pulses these states accumulate a phase related to their kinetic energy. This phase evolution is determined by the value of T, which therefore governs the type of dynamics exhibited by the system. As in Refs. [13,14], we use scaled dynamical variables $\chi = Gz$ and $\rho = GTp/m$. This defines an effective scaled, dimensionless Planck constant $k = -i[\hat{\chi}, \hat{\rho}] = \hbar G^2 T/m$, which together with ϕ_d and $\gamma = gGT^2$ (accounting for the effect of gravity) fully describes the quantum dynamics of the δ-kicked accelerator. When quantum resonances occur in the δ-kicked rotor ($\gamma = 0$), the phase difference accumulated between momentum states separated by $\hbar G$ from one pulse to the next is equal to an integer multiple of 2π. For a state of zero initial momentum, this is the case for

values of T corresponding to $\hbar k = 4\pi\ell$, where $\ell \in \mathbb{Z}$. This rephasing is analogous to the Talbot effect in optics [16], and so we speak of these resonances as occurring at integer multiples of the Talbot time $T_T = 4\pi m/\hbar G^2$ [12]. For a continuous initial distribution of momenta, such as in a cold atomic ensemble, resonant behavior is observed for $\hbar k = 2\pi\ell$, i.e., at integer multiples of the half-Talbot time $T_{1/2}$ [9,10,13]. Close to these values of T, QAM are found in the δ-kicked accelerator [13].

In our realization of the quantum δ-kicked accelerator, $\sim 10^7$ cesium atoms are trapped and cooled in a magneto-optic trap to ~ 5 μK, yielding a Gaussian momentum distribution with FWHM $6\hbar G$. The atoms are then released from optical molasses and, falling freely under gravity, are exposed to pulses from a vertical standing wave of laser light 20 GHz red-detuned from the $6\,^2S_{1/2} \rightarrow 6\,^2P_{1/2}$, $(F = 4 \rightarrow F' = 3)$ D1 transition. Hence, $\lambda_{\text{spat}} = 447$ nm and $T_{1/2} = 66.7$ μs. The intensity of the light is approximately 1×10^4 mW/cm^2, and the duration of each pulse is $t_p = 500$ ns. Through the action of the ac Stark shift, these pulses result in δ-function-like applications of a sinusoidal potential to the atoms, with $\phi_d = \Omega^2 t_p/8\delta_L$. Here Ω is the Rabi frequency, and δ_L is the detuning. Both the trapped atom density distribution and the standing light wave intensity profile are Gaussian, with FWHM of 1 mm. The resulting mean value of ϕ_d is $\sim 0.8\pi$. After application of the diffracting pulses, the atoms fall through a sheet of light resonant with the $6\,^2S_{1/2} \rightarrow 6\,^2P_{3/2}$, $(F = 4 \rightarrow F'' = 5)$ D2 transition, 0.5 m below the point of release, and their momentum distribution is measured by a time-of-flight technique with a resolution of $\sim\hbar G$. For more details, see Refs. [12–14].

The approach used by FGR [5] accounts for the observed acceleration of atoms participating in a QAM using trajectories in a map for a classical point particle. The validity of this map can be justified asymptotically by $\epsilon = (\hbar k - 2\pi\ell) \rightarrow 0$ (not $\hbar k \rightarrow 0$, hence the description pseudoclassical) or, equivalently, by $(\ell - T/T_{1/2}) \rightarrow 0$. In an appropriately transformed frame [5], the map is [14]

$$\tilde{p}_{n+1} = \tilde{p}_n - \tilde{k}\sin(\chi_n) - \text{sgn}(\epsilon)\gamma, \tag{2}$$

$$\chi_{n+1} = \chi_n + \text{sgn}(\epsilon)\tilde{p}_{n+1}, \tag{3}$$

where $\tilde{p} = p\epsilon/\hbar k$, and $\tilde{k} = \phi_d|\epsilon|$. Iteration of Eqs. (2) and (3) reveals systems of accelerator orbits. These are stable fixed points centered on islands in the pseudoclassical phase space. To yield an observable QAM, an island system must be sufficiently large, in terms of total phase-space area. Furthermore, the islands must be large, or at least comparable to $|\epsilon|$ (which takes the place of $\hbar$ as a measure of the size of a minimal "quantum phase-space" cell) for a point-particle-like description of the QAM dynamics to be appropriate. We show that when these requirements are satisfied the momentum gain predicted by the analysis of FGR agrees very well with experiment, even when $\hbar k$ is not extremely close to a resonant value. This can be understood as being due to the relevant dynamics taking place in stable regions of the pseudoclassical phase space, where semiclassical analyses can generally be expected to work reasonably well [17].

FGR [5] classify accelerator orbits (and thus QAM) by the order p of the fixed point (i.e., how many pulse periods it takes before cycling back to the initial point in the reduced phase-space cell) and the jumping index j (related to how many units of the momentum period of phase space are imparted per cycle). Particles in a (p, j) mode with initial momentum $q_0\hbar G$ have, after N kicks, momentum (in units of $\hbar G$)

$$q \simeq q_0 + \frac{N}{|\ell - T/T_{1/2}|}\left[\frac{j}{p} + \text{sgn}(\ell - T/T_{1/2})\frac{\gamma}{2\pi}\right], \tag{4}$$

in a frame accelerating with gravity. Only atoms of certain initial momenta will be accelerated [5,12]. As our initial atomic ensemble extends over many phase-space cells, all such conditions can be satisfied. Atoms fulfilling these conditions will receive the same momentum transfer, independent of the value of ϕ_d. Only the efficiency of populating a QAM varies with ϕ_d [12], and in our experimental arrangement the mean value of ϕ_d experienced by the atoms is sufficiently large (0.8π) to ensure an observable population in a large number of QAM. Since the mean initial momentum is 0, the central momentum of the observed QAM is well described by Eq. (4) with $q_0 = 0$.

To search for high-order QAM, we measured the momentum distribution after a fixed number of pulses for a range of T near the first three integer multiples of $T_{1/2}$. Figure 1 displays the momentum distributions after 30 pulses for values of T in the region of (a) $T_{1/2}$ ($T =$ 60.5 to 74.5 μs), (b) $T_T = 2T_{1/2}$ (124.5 to 142.5 μs), and (c) $3T_{1/2}$ (191.5 to 209.5 μs). The dotted curves indicate the theoretical predictions of Eq. (4). There is some disagreement for very large momenta, particularly large negative momenta. At these momenta, the atoms have left the Raman-Nath regime [13], moving so quickly that they travel a significant fraction of the standing wave period λ_{spat} during a pulse, and experience a spatially averaged potential. Such an effect will be stronger for atoms accelerated in the negative direction (*with* gravity) than in the positive (*against* gravity).

Certain of the more slowly accelerating (higher-order) QAM can be resolved only after applying a larger number of pulses than used in Fig. 1. To observe the emergence of several such modes, the value of T was scanned, for larger pulse numbers, in the region of T_T. Figure 2 shows the experimental momentum distributions after (a) 60, (b) 90, (c) 120, and (d) 150 pulses. Overlaid dotted lines indicate the predictions of Eq. (4). In Fig. 2(a) we can now identify the $(13, -5)$ and $(23, 9)$ modes. After 90 kicks [Fig. 2(b)] the $(18, -7)$ QAM is emerging, whereas the

momenta of the (2, 1) and the (5, −2) modes have grown beyond the measurable range. In Figs. 2(c) and 2(d) the atoms have received yet more momentum, and the (3, −1) mode is no longer visible. Note that some of the QAM seem to "fade" and become diffuse with time; this effect is not predicted by the pseudoclassical model and may be due to tunneling [5].

We now explicitly connect the observed high-order QAM around T_T, as displayed in Figs. 1(b) and 2, with their corresponding island systems in pseudoclassical phase space. Figure 3 shows stroboscopic phase-space plots, generated by repeated iterations of Eqs. (2) and (3), for different values of T around T_T. Comparing Figs. 2 and 3, we see that the appearance and disappearance of the QAM and of the stable island systems as T is varied coincide. The islands are robust to small variations in ϕ_d [14], meaning that the plotted phase spaces (corresponding to the mean value of $\phi_d = 0.8\pi$) give a reliable indication of which QAM will be observable, even though ϕ_d experimentally takes a range of values. Figure 3(a) ($T = 130.0\ \mu$s) shows the three large islands corresponding to the (3, −1) QAM. In Fig. 3(b) it is possible to observe the coexistence of a (5, −2) and a (8, −3) island system at $T = 132.2\ \mu$s, which can be seen to be consistent with the experimental results in Figs. 1(b) and 2(a). Interestingly, these yield simultaneous momentum transfer in opposite directions, promising application as a beam-splitting technique. Figure 3(c) ($T = 132.8\ \mu$s) shows the emergence of a (13, −5) accelerator orbit, while in Fig. 3(d) we see a complex (23, 9) island system at $T = 133.5\ \mu$s (just greater than T_T). This nevertheless

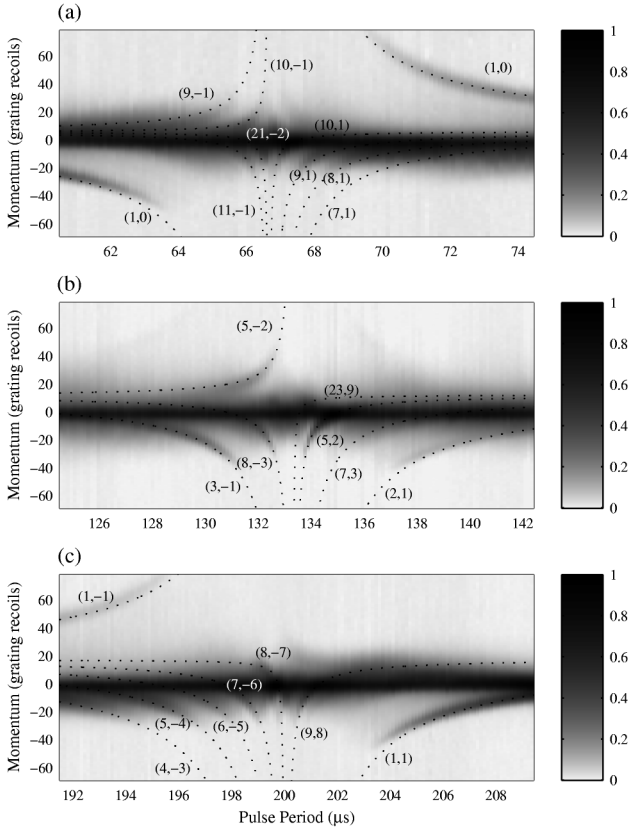

FIG. 1. Grey-scale plots of the variation with T of the experimental momentum distribution after 30 pulses, in a frame falling freely with gravity. The value of T is varied around (a) $T_{1/2}$, (b) $T_T = 2T_{1/2}$, and (c) $3T_{1/2}$, in steps of 0.128 μs. Dotted lines indicate the predicted momenta [Eq. (4)] of selected QAM, labeled (p, j). Population arbitrarily normalized to maximum value = 1.

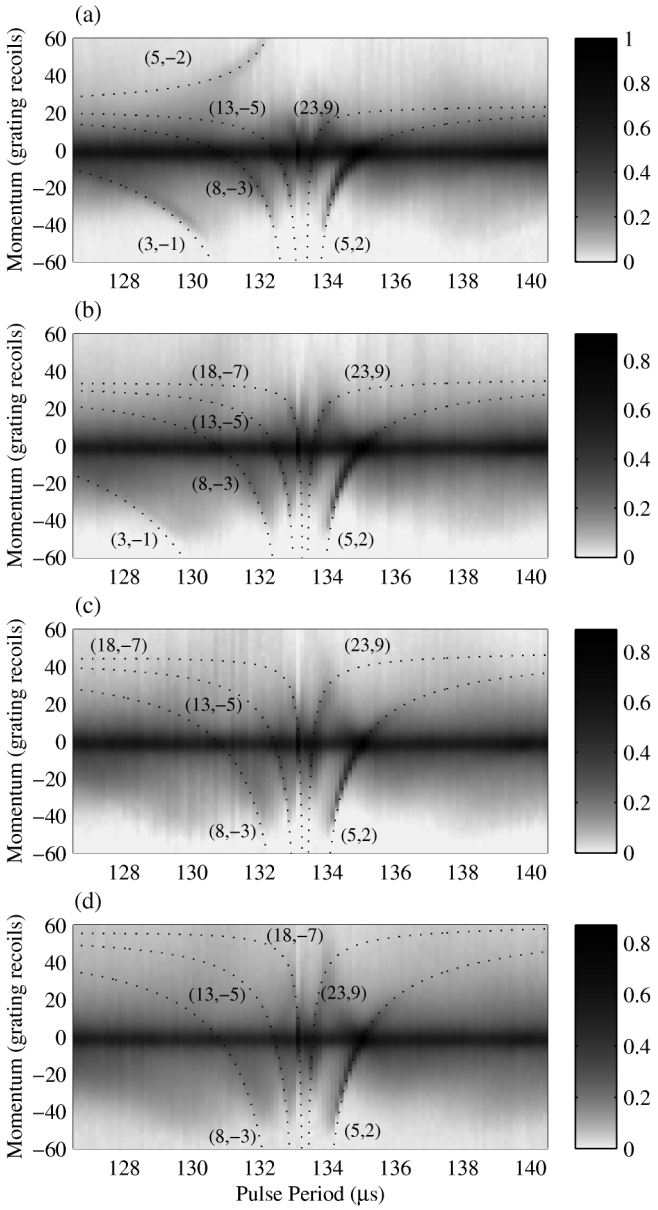

FIG. 2. Experimental momentum distributions for different pulse numbers as T is varied in the vicinity of T_T, from 124.5 to 142.5 μs in steps of 0.128 μs. The pulse number is (a) 60, (b) 90, (c) 120, and (d) 150. Dotted lines indicate the predicted momenta [Eq. (4)] of selected QAM, labeled (p, j). Population arbitrarily normalized to maximum value in subplot (a) = 1.

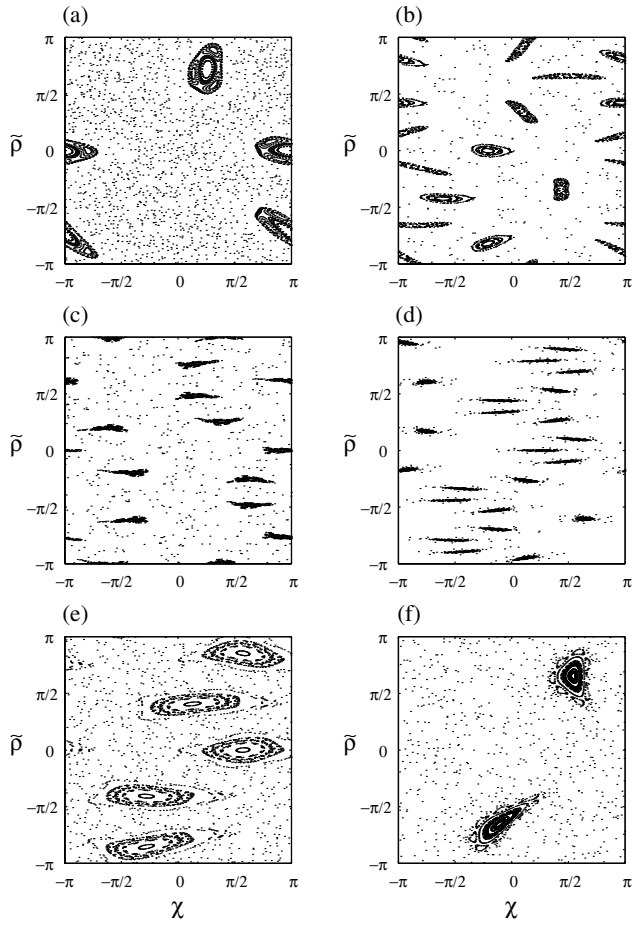

FIG. 3. Phase space plots produced by Eqs. (2) and (3) for T close to T_T. The islands correspond to the following QAM: (a) $T = 130.0\ \mu$s, and $(p, j) = (3, -1)$; (b) $T = 132.2\ \mu$s, $(p, j) = (5, -2)$ (shorter, rounder islands) and $(8, -3)$ (thin, elongated islands); (c) $T = 132.8\ \mu$s, $(p, j) = (13, -5)$; (d) $T = 133.5\ \mu$s, $(p, j) = (23, 9)$; (e) $T = 134.2\ \mu$s, $(p, j) = (5, 2)$; and (f) $T = 139.4\ \mu$s, $(p, j) = (2, 1)$. Initial conditions are clustered around the fixed points corresponding to accelerator orbits to highlight the structure of the island system of interest.

corresponds to a fairly robust QAM that is clearly visible in each of the subplots of Fig. 2. Moving further away from T_T, in Figs. 3(e) and 3(f) ($T = 134.2$ and $139.4\ \mu$s, respectively), we again observe comparatively simple $(5, 2)$ and $(2, 1)$ orbits.

In conclusion, we have successfully observed a multitude of quantum accelerator modes of up to 23rd order and connected them to the periodic orbits of a classical map. This was derived by FGR [5] as a pseudoclassical limit of the underlying quantum dynamics when the pulse period approaches certain resonance times. Linking this theory with our experiment, we have successfully performed quantum accelerator mode spectroscopy. Confirmation of the validity of such a theoretical approach promises new avenues for investigation of quantum-classical correspondence in a chaotic context. Furthermore, the efficient momentum transfer occurring in these atomic dynamics is of great intrinsic interest. We have recently demonstrated quantum accelerator modes to be formed coherently [14], and the simultaneous existence of quantum accelerator modes in opposite momentum directions could be applied as a beam splitter for large-area atom interferometry [18].

We thank R. Bach, K. Burnett, S. Fishman, I. Guarneri, L. Rebuzzini, and S. Wimberger for stimulating discussions. We acknowledge support from the UK EPSRC, the Paul Instrument Fund of The Royal Society, and the EU through the TMR "Cold Quantum Gases" network.

[1] *New Directions in Quantum Chaos*, edited by G. Casati, I. Guarneri, and U. Smilansky (IOS Press, Amsterdam, 2000).
[2] M. C. Gutzwiller, *Chaos in Classical and Quantum Mechanics* (Springer-Verlag, New York, 1990).
[3] F. Haake, *Quantum Signatures of Chaos* (Springer-Verlag, Berlin, 2001), 2nd ed.
[4] L. E. Reichl, *The Transition to Chaos in Conservative Classical Systems: Quantum Manifestations* (Springer-Verlag, New York, 1992).
[5] S. Fishman, I. Guarneri, and L. Rebuzzini, Phys. Rev. Lett. **89**, 084101 (2002); J. Stat. Phys. **110**, 911 (2003).
[6] F. M. Izrailev and D. L. Shepelyanskii, Sov. Phys. Dokl. **24**, 996 (1979).
[7] G. Casati *et al.*, in *Stochastic Behaviour in Classical and Quantum Hamiltonian Systems* (Springer-Verlag, New York, 1979).
[8] F. L. Moore *et al.*, Phys. Rev. Lett. **75**, 4598 (1995).
[9] W. H. Oskay *et al.*, Opt. Commun. **179**, 137 (2000).
[10] M. B. d'Arcy *et al.*, Phys. Rev. Lett. **87**, 074102 (2001).
[11] M. K. Oberthaler *et al.*, Phys. Rev. Lett. **83**, 4447 (1999).
[12] R. M. Godun *et al.*, Phys. Rev. A **62**, 013411 (2000).
[13] M. B. d'Arcy *et al.*, Phys. Rev. E **64**, 056233 (2001).
[14] S. Schlunk *et al.*, Phys. Rev. Lett. **90**, 054101 (2003).
[15] B. G. Klappauf *et al.*, Phys. Rev. Lett. **81**, 1203 (1998); H. Ammann *et al.*, *ibid.* **80**, 4111 (1998); W. K. Hensinger *et al.*, Nature (London) **412**, 52 (2001); D. A. Steck, W. H. Oskay, and M. G. Raizen, Science **293**, 274 (2001).
[16] See also related work on classical optics by M.V. Berry and E. Bodenschatz, J. Mod. Opt. **46**, 349 (1999).
[17] W. H. Zurek and J. P. Paz, Phys. Rev. Lett. **72**, 2508 (1994).
[18] P. Berman, *Atom Interferometry* (Academic, San Diego, 1997).